# Supporting Information

# Large-Area Aligned Fullerene Nanocrystal Scaffolds as Culture Substrates for Enhancing Mesenchymal Stem Cell Self-Renewal and Multipotency

*Jingwen Song,*[†] *Xiaofang Jia,*[*,‡] *Kosuke Minami,*[†,§,⊥] *Jonathan P. Hill,*[‡] *Jun Nakanishi,*[‡] *Lok Kumar Shrestha,*[‡] *Katsuhiko Ariga*[*,†,‡]

[†]Graduate School of Frontier Sciences, The University of Tokyo, 5-1-5 Kashiwanoha, Kashiwa, Chiba 277-8561, Japan.

[‡]International Research Center for Materials Nanoarchitectonics (MANA), National Institute for Materials Science (NIMS), 1-1 Namiki, Tsukuba, Ibaraki 305-0044, Japan.

[§]International Center for Young Scientists (ICYS), National Institute for Materials Science (NIMS), 1-1 Namiki, Tsukuba, Ibaraki 305-0044, Japan.

[⊥]Center for Functional Sensor and Actuator (CFSN), National Institute for Materials Science (NIMS), 1-1 Namiki, Tsukuba, Ibaraki 305-0044, Japan.

**Corresponding Author**

*E-mail: JIA.Xiaofang@nims.go.jp

*E-mail: ARIGA.Katsuhiko@nims.go.jp

**Table S1.** Representative stem cell expansion using different strategies.

| **Materials** | **Carbon nanotube** | **Polyethylene glycol** | **Polycaprolactone** | **Elastin-like protein** | **Fullerene** |
|---|---|---|---|---|---|
| Works | ACS Appl. Mater. Interfaces 2014,6, 2598 | Science 2010, 329, 1078 | Nat. Mater. 2011, 10,637 | Nat. Mater. 2017, 16,1233 | **This work** |
| Method | Deposited | Elastic substrate | Electron beam lithography | Degradable substrate | **LB** |
| Nanotopography | ✓ | × | ✓ | × | ✓ |
| Large area | ✓ | × | × | × | ✓ |
| Cell shape control | × | × | ✓ | × | ✓ |
| High Proliferation | × | ✓ | ✓ | × | ✓ |
| Simple preparation | ✓ | × | × | × | ✓ |
| Low cost | ✓ | × | × | × | ✓ |
| Biocompatibility | × | ✓ | ✓ | ✓ | ✓ |

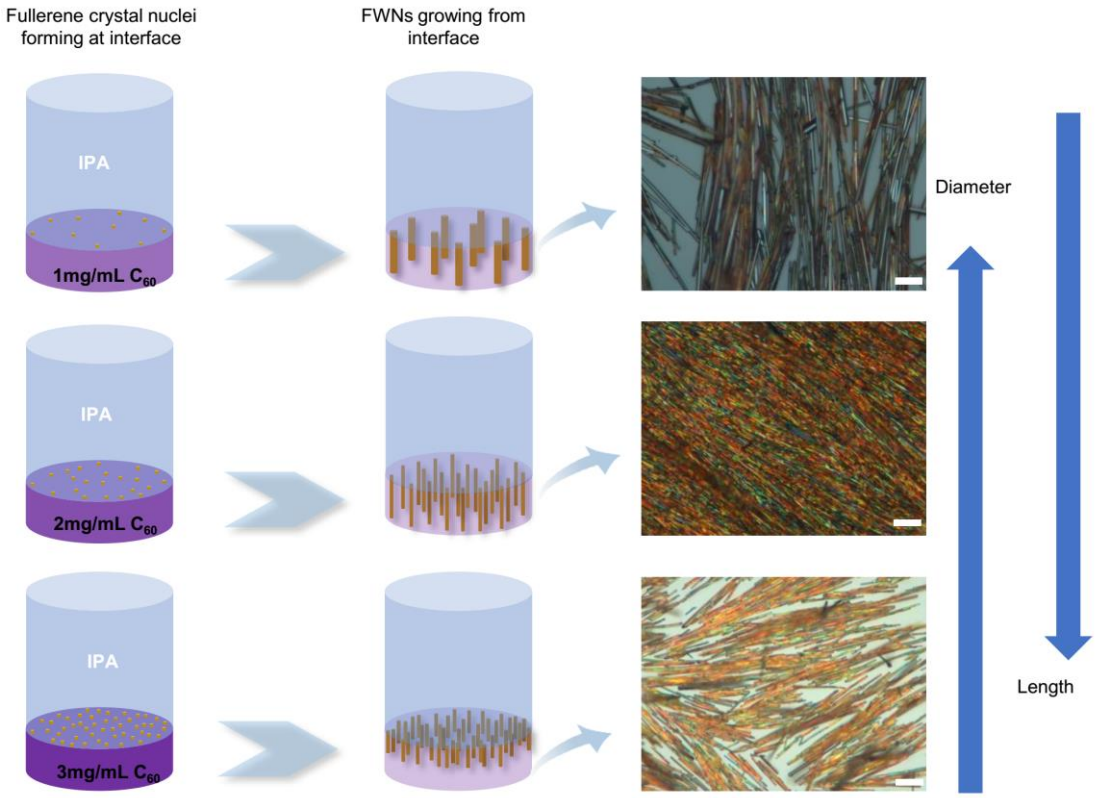


**Figure S1.** Photomicrographs of FNWs prepared using different concentrations of $C_{60}$ dissolved in m-xylene. Concentration of $C_{60}$ solutions in m-xylene was selected (1 mg/mL, 2 mg/mL and 3 mg/mL) for the regulation of the supramolecular assembly process. Scale bars: 20 μm. At higher concentrations of $C_{60}$ solution (3 mg/mL), a greater number of nuclei were formed at the liquid–liquid interface resulting in shorter FNWs with a highly uniform morphology. At lower concentration of $C_{60}$ solution (1 mg/mL), fewer nuclei were formed at liquid–liquid interface leading to longer FNWs with lower uniformity of morphology. To obtain long FNWs with uniform morphology, a static liquid–liquid interfacial precipitation method using 2 mg/mL $C_{60}$ stock solution was used for supramolecular assembly.

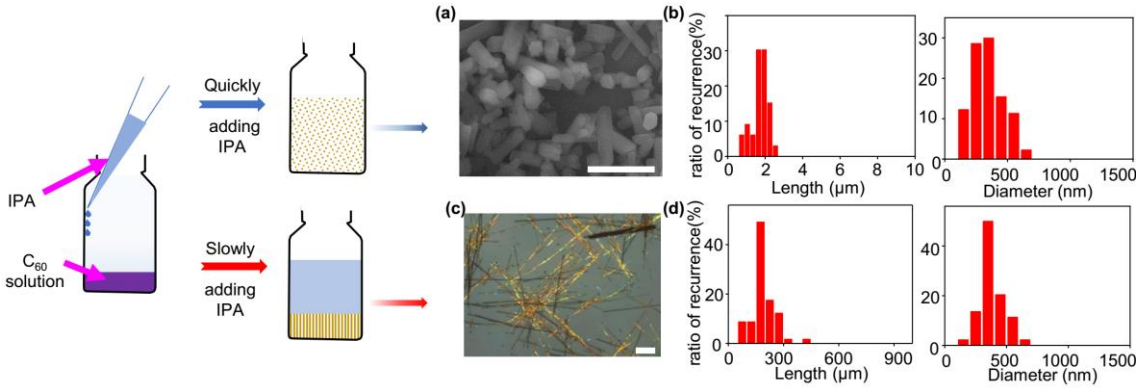


**Figure S2.** Experimental method (at right) with micrographs and size distributions of low-aspect-ratio and high-aspect-ratio FNWs. (a) SEM image of low-aspect-ratio FNWs. Scale bar: 2 μm. (b) Histograms for lengths and diameters of low-aspect-ratio FNWs. (c) Photomicrograph of high-aspect-ratio FNWs. Scale bar: 50 μm. (d) Histograms for lengths and diameters of high-aspect-ratio FNWs.

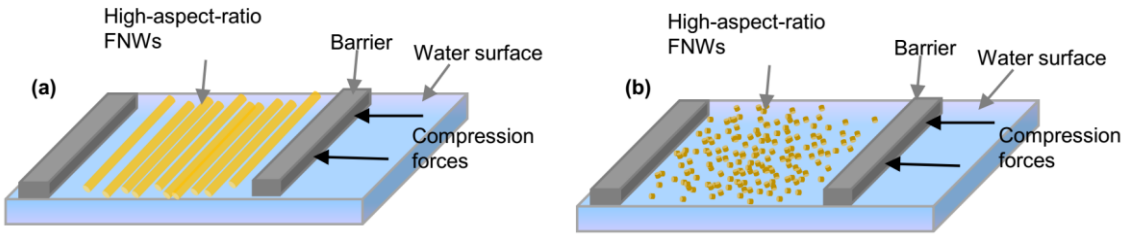


**Figure S3.** Schematic illustration of of the guided assembly of FNWs using the LB approach. (a) High-aspect-ratio FNWs and (b) low-aspect-ratio FNWs floating at a water surface form high density FNWs monolayer under compression.

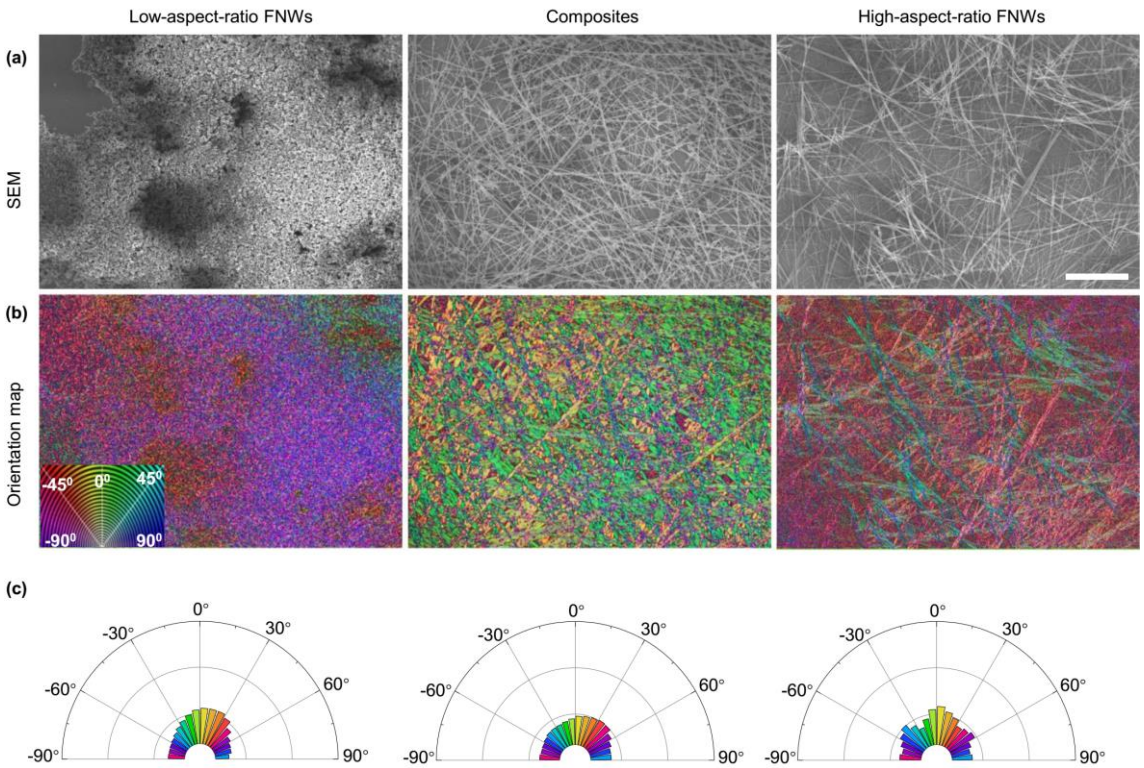


**Figure S4.** FNWs coated on a glass substrate by drop-casting. SEM images (a) corresponding orientation-color-coded images (b) and angular distribution (c) of low-aspect-ratio FNWs (left), high-aspect-ratio FNWs (right) and a composite with the weight ratio of low- and high- aspect-ratio FNWs of 3 (middle). Inset in the left panel of (b) shows the color code for orientation (different colors indicate different orientation directions). Scale bar: 40 μm.

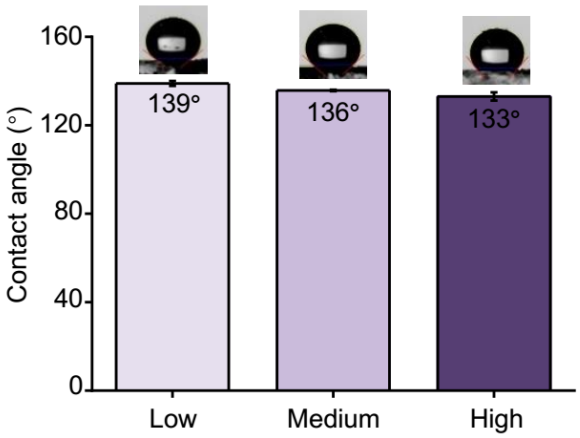


**Figure S5.** Wettability analysis of low-, medium-, and high-aFNWs nanopatterned scaffolds. Contact angle images and values for water droplet on different aFNWs patterned scaffolds. *n* = 5, mean ± s.d.

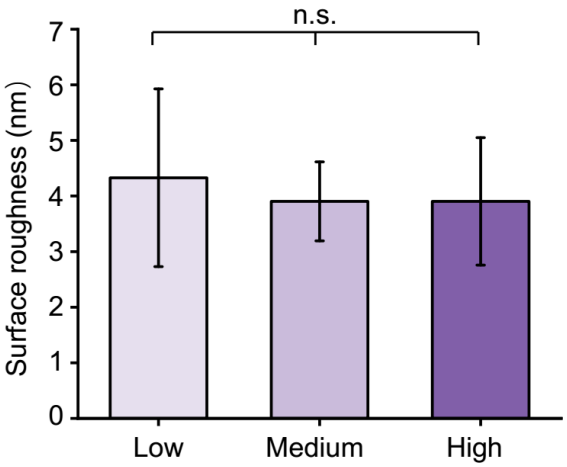


**Figure S6.** Root-mean-squared (rms) surface roughness of low-, medium-, and high-aFNWs nanopatterned scaffolds. $n$ = 15, mean ± s.d.

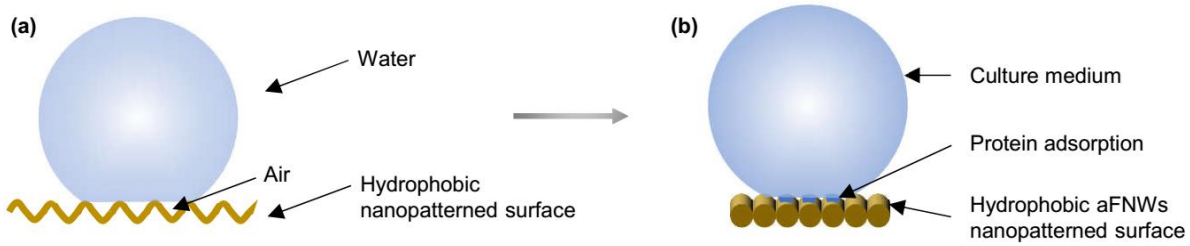


**Figure S7.** Schematic illustration of protein adsorption on hydrophobic aFNWs nanopatterned scaffold. (a) Cassie model of hydrophobic nanopatterned surface. Surface roughness or topography has a significant influence on the surface energy. Hydrophobic nanopatterned surfaces having water-repellent properties prevent water from contacting the entire surface. (b) aFNWs scaffold promotes formation of a protein pattern on the ridges of aFNWs.

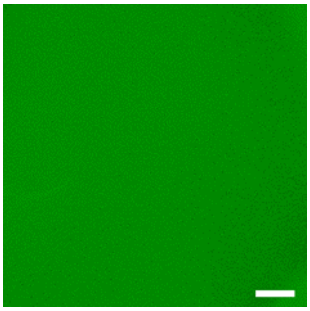

**Figure S8.** Protein adsorption on glass. Fluorescence image of bare glass soaked in 0.1 mg/mL fluorescent labelled fibronectin solution in PBS for 1 h. Scale bar: 25 μm.

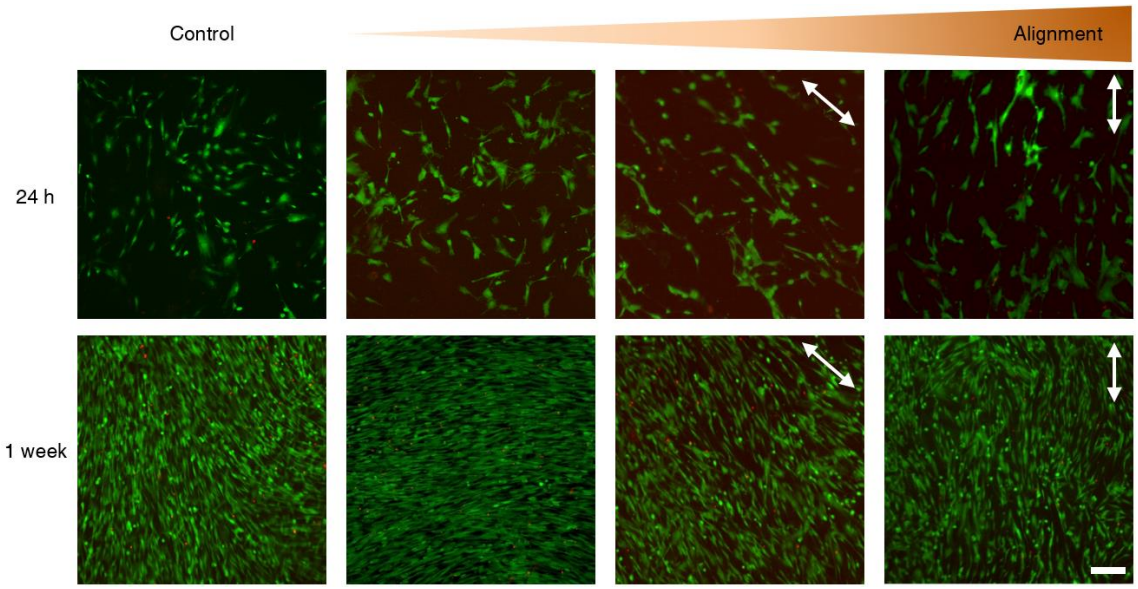


**Figure S9.** hMSCs viability on aFNWs scaffolds and glass. LIVE/DEAD assay of hMSCs cultured on low-, medium-, and high-aFNWs scaffolds after 24 h and 1 week. hMSCs cultured on bare glass surface as control (panels at left). Live hMSCs labeled with calcein AM (green) and dead hMSCs labeled with EthD-1(red). White arrow indicates the pattern direction. Scale bar: 200 μm.

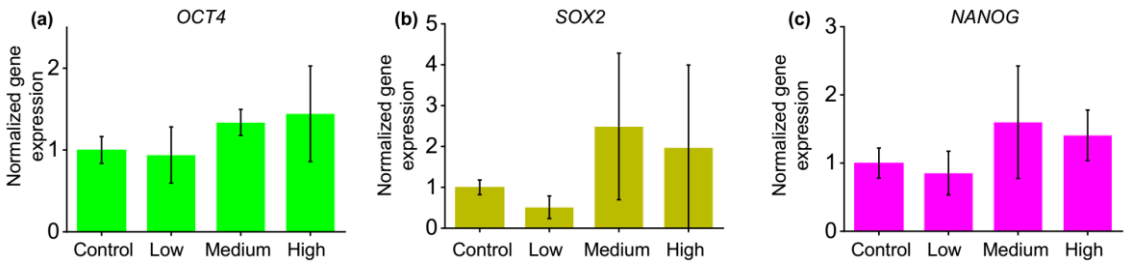


**Figure S10.** qRT-PCR analysis of the expression of hMSCs stemness markers after 1 week. *OCT4* (a), *SOX2* (b) and *NANOG* (c) expression of hMSCs cultured on low-, medium-, and high-aFNWs nanopatterned scaffolds. hMSCs cultured on glass surface as control. Normalized gene expression to control group. $n = 3$, mean ± s.d.

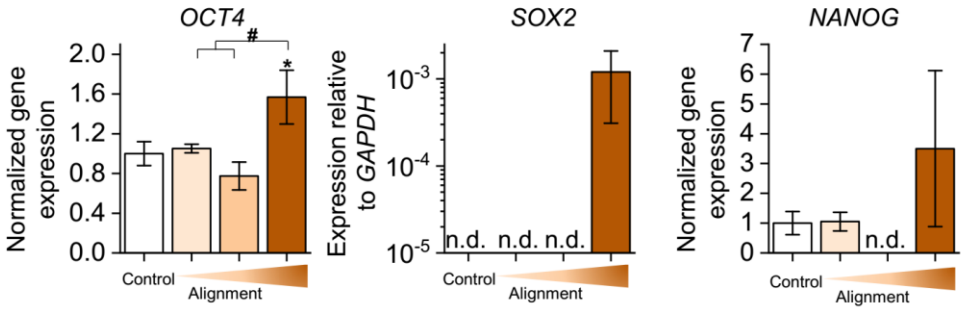


**Figure S11.** qRT-PCR analysis of stemness markers *OCT4*, *SOX2* and *NANOG* after 2 weeks. hMSCs (bone marrow, Lonza) were cultured in standard growth medium (Lonza). *OCT4* and *NANOG* gene expression is normalized against cells cultured on glass. The relative expression of *SOX2* was compared with *GAPDH*. $n = 3$, mean ± s.d., n.d.: not detected, $^{*}P < 0.05$ vs. control, $^{\#}P < 0.05$, two-tailed Student's *t*-test.

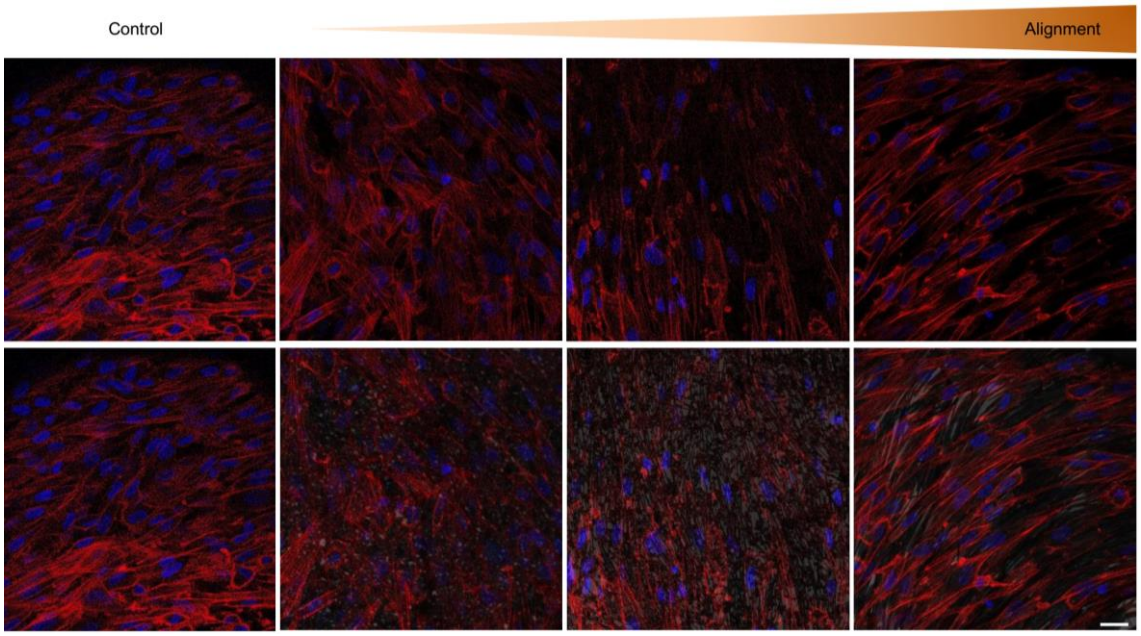


**Figure S12.** Morphologies of hMSCs cultured on aFNWs scaffolds after 2 weeks. Representative fluorescence images of hMSCs cultured on the surface of low-, medium- and high-aFNWs nanopatterned scaffolds (F-actin in red, nucleus in blue). Lower panels also show bright field in gray. Panels at left show hMSCs cultured on bare glass surface as control.

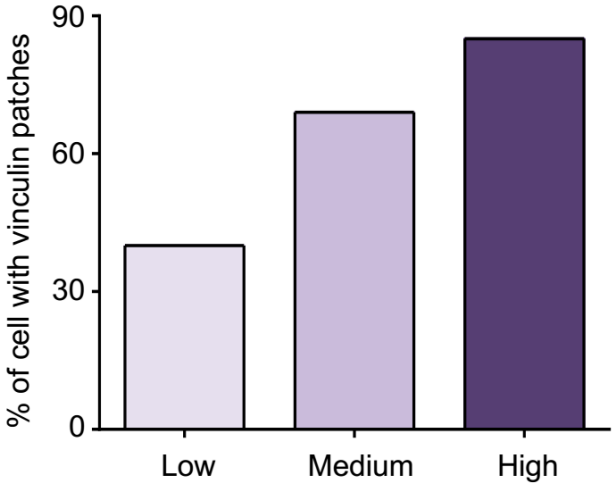


**Figure S13.** Percentage of hMSCs with vinculin patches on low-, medium- and high-aFNWs nanopatterned scaffolds. $n$ = 10–13 cells.